

1 **A Data-Driven Approach for Daily Real-Time Estimates and Forecasts**
2 **of Near-Surface Soil Moisture**

3
4 Randal D. Koster¹, Rolf H. Reichle¹, and Sarith P. P. Mahanama^{1,2}

5 ¹Global Modeling and Assimilation Office, NASA/GSFC, Greenbelt, Maryland

6 ²Science Systems and Applications, Inc., Lanham, Maryland

7
8
9 Corresponding author:

10 Randal Koster

11 Code 610.1, NASA/GSFC

12 Greenbelt, MD 20771

13 randal.d.koster@nasa.gov

14 301-614-5781

17

18

Abstract

19 NASA's Soil Moisture Active Passive (SMAP) mission provides global surface soil moisture
20 retrievals with a revisit time of 2-3 days and a latency of 24 hours. Here, to enhance the utility of
21 the SMAP data, we present an approach for improving real-time soil moisture estimates
22 ("nowcasts") and for forecasting soil moisture several days into the future. The approach, which
23 involves using an estimate of loss processes (evaporation and drainage) and precipitation to
24 evolve the most recent SMAP retrieval forward in time, is evaluated against subsequent SMAP
25 retrievals themselves. The nowcast accuracy over the continental United States (CONUS) is
26 shown to be markedly higher than that achieved with the simple yet common persistence
27 approach. The accuracy of soil moisture forecasts, which rely on precipitation forecasts rather
28 than on precipitation measurements, is reduced relative to nowcast accuracy but is still
29 significantly higher than that obtained through persistence.

30

31

32

33 **1. Introduction**

34 The SMAP (Soil Moisture Active Passive, Entekhabi et al. 2010) mission provides estimates,
35 across the globe, of moisture in the top several centimeters of soil at a spatial resolution of about
36 40 km and with a revisit time of 3 days or less. To promote the use of the data in the community,
37 the data are produced with a mean latency of 24 hours, close to real time for many applications.
38 We posit, as motivation for the present paper, that some users of these data may find utility in
39 products of even lower latency (soil moisture “nowcasts”, i.e., with a latency of 0 hours) as well
40 as in soil moisture forecasts, out several days. Such information could benefit, for example,
41 those who use soil moisture to evaluate current and near-future ground trafficability or the
42 potential for certain hazards such as flash floods and landslides.

43 The objective of this paper is to describe an approach for deriving improved real-time and
44 forecasted surface soil moisture estimates from the SMAP data. Given a soil moisture retrieval,
45 W_N , on Day N, our approach considers the forward evolution of soil moisture from this value
46 using precipitation estimates (either measured or forecasted) in combination with a loss function,
47 the latter being derived from a history of SMAP retrievals and precipitation observations. The
48 resulting real-time and forecasted soil moisture estimates are thus data-driven (independent of
49 land model formulation) and are statistically consistent with the original retrieval product,
50 greatly facilitating their use in applications that already utilize near-real time SMAP data, at least
51 in areas with adequate precipitation data. (The approach will not provide reliable soil moisture
52 estimates where precipitation is poorly measured.)

53 The datasets used here and the estimation approach are described in section 2. The accuracy of
54 the estimates so produced is illustrated in section 3 through quantitative comparisons with
55 subsequent SMAP retrievals. For context, this accuracy is compared to that obtained with an
56 approach already applied, knowingly or not, by many data users: assuming simple persistence,
57 i.e., assuming that the best estimate of the current soil moisture state is the most recently
58 measured value for that state, even if that measurement is a day to several days old.

59

60 **2. Data and Approach**

61

62 a. Datasets Used

63 We use SMAP Version 3 Level 2 soil moisture retrievals (O'Neill et al. 2016; Jackson et al.
64 2016), which are based on L-band radiometer measurements. These data represent volumetric
65 soil moisture in roughly the top 5 cm of soil and are provided on a 36 km equal-area Earth-fixed
66 grid (Brodzik et al. 2012). As in Koster et al. (2016), we ignore the retrieval flag associated with
67 “recommended quality” to allow greater spatial and temporal coverage.

68 The precipitation data used to derive the soil moisture loss functions are from the Climate
69 Prediction Center Unified Gauge-Based Analysis of Global Daily Precipitation (CPCU;

70 ftp://ftp.cpc.ncep.noaa.gov/precip/CPC_UNI_PRCP/GAUGE_GLB/). As in Koster et al. (2016),
71 this $0.5^\circ \times 0.5^\circ$ dataset was converted to the SMAP grid using a conservative regriding (areal
72 weighting) approach. In CONUS, a precipitation amount listed for a given day corresponds to
73 water falling over the 24 hours up to 12Z on that day; 12Z corresponds to 6AM in the middle of
74 the country, the approximate local solar time of the SMAP retrievals.

75 The 2016 precipitation forecasts (also regrided to the SMAP grid) are from the Goddard Earth
76 Observing System, Version 5.13.1 (GEOS-5) model
77 (https://gmao.gsfc.nasa.gov/GMAO_products). For each day considered in the evaluation phase
78 of the study (May-September of 2016; see below), precipitation forecasts from GEOS-5 are
79 available for the following 5 days beginning at 12Z.

80

81 b. Estimation Approach

82 In the following, we assume that a SMAP soil moisture retrieval (in volumetric units, m^3/m^3) for
83 Day N, W_N , is available on Day N+1 (given the 24-hour latency) and that we require estimates of
84 W_{N+1} through W_{N+5} . (For example, if the current day is N+1, we require a “nowcast” of soil
85 moisture on that day as well as soil moisture forecasts for the next four days based on the
86 previous day’s measurement W_N .) Our approach involves updating W through those five days
87 by integrating equations that address how soil moisture increases with precipitation and

88 decreases with evapotranspiration and drainage. Given a SMAP retrieval on Day N, we update
89 soil moisture over the next five days (hour by hour) with:

$$90 \quad W(t+\Delta t) = W(t) - L(W(t)) \cdot \Delta t + W_{\text{add}}, \quad (1)$$

91 where t is the hour of integration, the time step Δt is set to 3600 s, and $L(W(t))$ is the assumed
92 rate of soil moisture loss via evapotranspiration and drainage (volumetric units per second). The
93 term W_{add} is the soil moisture increase associated with I (mm/s), the assigned infiltration rate:

$$94 \quad W_{\text{add}} = I \Delta t / D, \quad (2)$$

95 where the depth D is set to 50 mm and W_{add} is thus in volumetric units. The infiltration rate I is
96 in turn set equal to the measured or forecasted precipitation rate P (mm/s) unless that rate, if it
97 were to be applied over a full day, would exceed the current soil water deficit:

$$98 \quad I = \min \{ P, D(W_{\text{max}} - W(t)) / n_d \}, \quad (3)$$

99 where n_d is the number of seconds in a day and W_{max} is the assumed maximum allowable value
100 for W . If I is set to the second term (associated with the soil water deficit) in (3), the excess
101 precipitation water is assumed to run off the surface. The somewhat arbitrary use of a daily total
102 to determine the excess reflects in part our lack of knowledge of the sub-diurnal character of the
103 daily precipitation.

104 The precipitation rate P is taken from observations (to the extent possible, up to the present time)
105 or from a weather forecast model. Test runs were performed to verify that an hourly time step
106 for the integration of the equations is indeed adequate; the results presented in section 3 below
107 are essentially reproduced when the time step is decreased, for example, to 6 minutes.

108

109 c. Loss Function Estimation

110 Using (1)-(3) to update soil moisture requires a description of the loss function L and an estimate
111 for W_{\max} . For this we jointly analyze SMAP soil moisture retrievals and CPCU precipitation
112 measurements during May-September 2015. At each grid cell, we determine the lowest and
113 highest soil moisture retrieval values, W_{low} and W_{high} , attained at that cell during that period.
114 The low end of the assumed soil moisture range, W_{\min} , is set to W_{low} , and the high end of the
115 range, W_{\max} , is arbitrarily set to $W_{\text{high}} + 0.1*(W_{\text{high}}-W_{\min})$. We set the value of the loss function
116 at the low end, $L(W_{\min})$, to 0. At W_{\max} , we set it to an arbitrarily high value: $L(W_{\max})=W_{\max}$
117 volumetric units per day. Note that such a high loss rate cannot be maintained for long – in our
118 simulations with L , unrealistic soil moistures at the high end quickly adjust themselves to
119 produce loss rates of reasonable magnitude. We tested different high values for $L(W_{\max})$ and
120 different definitions for W_{\max} , with little impact on our results.

121 We next identify the three intermediate soil moisture values (W_A , W_B , and W_C) that divide the
122 range between W_{\min} and W_{\max} into four equal segments. Estimating the loss function amounts to

123 determining L at these intermediate moistures; once these values are determined, the value of L
124 at any other soil moisture can be estimated through linear interpolation. We establish the optimal
125 values of $L(W_A)$, $L(W_B)$, and $L(W_C)$ through brute force. To test a set of L values at a given grid
126 cell, we initialize an integration with the first SMAP retrieval at the cell in May 2015 and use
127 (1)-(3) along with the 2015 gauge-based precipitation data to produce a time series of soil
128 moisture spanning May-September of that year, and we then compute the root mean square error
129 (RMSE) between the simulated soil moistures and the SMAP retrievals in the cell as they occur.
130 (Note that we could have chosen in these integrations to reset $W(t)$ to the SMAP retrieval values
131 as they occurred, after noting the error; tests indicate, however, that this modification has very
132 little impact on our results.) We test a comprehensive suite of $L(W_A)$, $L(W_B)$, and $L(W_C)$ values
133 in this way, limiting the search space by assuming that L never decreases with increasing soil
134 moisture, and find the one set that best reproduces the SMAP retrieval time series.

135 Figure 1 displays the loss functions derived at three representative interior sites. For each site,
136 the leftmost panel shows the optimized loss function itself, and the top right panel shows the
137 time series (covering May-September 2015) of the SMAP Level 2 retrievals there (as red dots) as
138 well as the soil moisture estimates (blue dots) derived with (1)-(3) using the loss function in
139 conjunction with CPCU rainfall data. For reference, the rainfall data are shown in the bottom
140 right panel.

141 Although they have the same basic form, the loss functions at the three sites differ, with larger
142 soil moisture losses occurring, for example, at low soil moistures for the New Mexico site
143 relative to the Arkansas site. The comparisons of the retrievals with the estimated soil moistures

144 generally show strong agreement in terms of RMSE and the square of the correlation coefficient
145 (r^2), indicating that the loss functions do indeed capture the hydrological behavior of the near-
146 surface soil. Again, these are representative results for the interior of CONUS; as shown in
147 Figure 2, however, the r^2 values are a bit lower, and thus the optimization of L is more
148 questionable, in the wet and highly vegetated areas of the East (perhaps due to the quality of the
149 SMAP retrievals under thick vegetation) and in the very dry areas of the Southwest (perhaps due
150 to irrigation impacts or to the low variability of soil moisture there during summer).

151 The concept of loss functions has an extensive history (e.g., Manabe, 1969). Direct estimates of
152 loss functions from observations are rare, but where they exist, it is encouraging to note that they
153 have the same basic form as those shown in Figure 1, with an increase in L with soil moisture at
154 the very dry end, a plateauing out of the relationship in the midrange (as in Figure 1b and 1c),
155 and a high sensitivity of L to soil moisture at the wet end (see, e.g., Salvucci et al. 2001, their
156 Figure 3; Sun et al. 2011, their Figure 2). Such functions in the literature are sometimes
157 normalized by net radiation or potential evaporation to account for seasonal variations in the
158 drivers of surface evaporation; we reduce the need for this here (and also mitigate snow cover
159 issues) by focusing on the May-September period over CONUS.

160

161 d. Simulations Performed and Accuracy Metric

162 We evaluate soil moisture nowcast and forecast skill obtained with our approach during May-
163 September of 2016, a period independent of that used (May-September of 2015) to estimate the
164 loss function L at each site. For each SMAP retrieval at each location, we integrate (1)-(3)
165 forward in time 5 days (starting with the retrieval value) using two sets of precipitation
166 estimates: (i) precipitation forecasts from the GEOS-5 modeling system, and (ii) CPCU rainfall
167 measurements, the type of data that might be available for producing soil moisture nowcasts.
168 We then compare the resulting soil moisture updates to any later SMAP retrievals appearing
169 during the 5-day window. For example, a grid cell with a SMAP retrieval on both Day N and
170 Day $N+3$ effectively produces a data pair ($[W_{\text{estimated}}(N+3), W_{\text{retrieved}}(N+3)]$) that can be included
171 in a 3-day-lead RMSE calculation. We compute the RMSE over all such 3-day-lead data pairs
172 during May-September of 2016. We similarly compute the RMSE for the other leads; at a given
173 grid cell, each RMSE will be based on a unique collection of dates. Naturally, our interpretation
174 of accuracy here is tempered by the knowledge that SMAP soil moisture retrievals have their
175 own errors; we are, in effect, quantifying the skill in predicting a SMAP retrieval before it is
176 available.

177 Our analyses focus on CONUS (including neighboring parts of Canada and Mexico), a large-
178 scale area with two important features: (i) precipitation measurements of suitable spatial and
179 temporal coverage, and (ii) climatic regimes that range from very dry (in the west) to wet and
180 humid (in the east).

181

182 **3. Results**

183 For a lead of one day, the leftmost and middle panels of Figure 3a show the accuracy of near-
184 surface soil moisture estimates produced with (1)-(3) using, for P, gauge-based rainfall data and
185 precipitation forecasts, respectively. For context, the rightmost panel shows the results obtained
186 by assuming soil moisture persistence, i.e., by assigning the value of the soil moisture retrieval
187 on day N to each of the subsequent five days. The next three rows show the corresponding
188 results for leads of 2, 3, and 5 days. Results for a 4-day lead are not shown; the number of
189 retrievals separated by exactly 4 days is severely limited over the US due to the orbital
190 characteristics of the SMAP observatory.

191 As expected, soil moisture estimates are more accurate when CPCU data rather than precipitation
192 forecasts are used in (1)-(3). Of course, the accuracy levels in the first column are only relevant
193 to nowcasts, and only in areas where real-time rainfall measurements are in fact available.
194 CPCU data are generally available to users with a latency of 1-2 days, which is relatively high.
195 We expect, however, that users in many areas will have more immediate access to local rainfall
196 measurements for local nowcast calculations, and some satellite-based precipitation datasets
197 have low latencies and may prove useful for the nowcasts – some components of the IMERG
198 product (Huffman et al., 2014), for example, feature a latency of several hours. If precipitation
199 measurements of any kind are not available, soil moisture nowcasts will need to rely on
200 precipitation forecasts (or analyzed precipitation products), and all soil moisture forecasts must
201 rely on precipitation forecasts; for these, the second column in Figure 3 is more relevant. Note
202 that for some estimations, measured precipitation may be available during the first part of the

203 simulation, in which case the relevant accuracies would lie in between the first and second
204 columns.

205 At all leads, RMSE values obtained with the loss function approach tend to lie below $0.04 \text{ m}^3/\text{m}^3$
206 in the western part of the continent and in areas along the eastern coast, using either rainfall
207 dataset. The higher RMSEs obtained with the loss function approach when using forecasted
208 rainfall still lie below $0.06 \text{ m}^3/\text{m}^3$ over most of the continent, particularly for leads of 3 days or
209 less. To provide some perspective, the SMAP mission imposes an accuracy requirement of 0.04
210 m^3/m^3 , though this is for evaluations against in situ data, something not attempted here.

211 Using either rainfall dataset, the RMSE values of our soil moisture estimates are lower almost
212 everywhere, for all leads, than those obtained with the persistence approach. Again, the
213 persistence approach is effectively employed by anyone who uses the most recent SMAP
214 retrieval in their particular application. Figure 3 suggests that using the loss function approach
215 instead for the application could prove beneficial.

216 The results are summarized in Figure 4, which shows the average RMSE computed across the
217 area at each lead for the different approaches. Again, using gauge-based precipitation in (1)-(3)
218 produces more accurate estimates than using precipitation forecasts, and both sets of estimates
219 outperform persistence. While persistence performs about as well as the loss function approach
220 with forecasted precipitation at a lead of one day (soil moistures do take some time to diverge
221 from initial values), the accuracy decreases relatively quickly with lead.

223 **4. Summary and Discussion**

224 The nowcasts and forecasts described in section 3 are fair, not being based on information from
225 the period following the retrieval. As seen in Figures 3 and 4, integrating (1)-(3) forward in time
226 produces nowcasts or forecasts that are more accurate – at least in terms of being able to predict
227 the next SMAP retrieval – than those obtained by assuming persistence.

228 Damped persistence, in which a soil moisture anomaly evolves with an assigned time scale
229 toward a climatological value during the forecast period, is another estimation approach, one that
230 can be tested once the SMAP data record is large enough to provide a reliable climatology.

231 Alternatively, real-time or forecasted soil moistures could be extracted directly from weather
232 forecast products. The approach described here, however, has some notable advantages. Unlike
233 damped persistence, the loss function approach, which implicitly uses locally-optimized damping
234 time scales, also makes use of measured or forecasted precipitation information. Unlike weather
235 forecast model soil moisture products, which are subject to inaccuracies in model formulation
236 and are characterized, in any case, by model-dependent statistical moments (Koster et al. 2009),
237 our approach makes direct use of the most recent SMAP retrieval and produces data that are, by
238 construction, statistically consistent with SMAP retrievals and are thus immediately relevant to
239 applications already using SMAP data. Note, however, that raw precipitation forecasts generated
240 with numerical weather prediction models can have statistics in conflict with those of the true
241 precipitation at a site (e.g., due to differences in spatial scale), and such deficiencies could affect

242 the statistics of the loss function-based soil moisture forecasts discussed herein. As a remedy,
243 the forecast precipitation rates could be suitably adjusted with established procedures (e.g., Clark
244 et al. 2004, Charba and Samplatsky 2011).

245 Another important caveat is the fact that the soil moisture estimation approach described herein
246 is limited to regions with adequate precipitation estimates, necessary for the construction of
247 accurate loss functions. Note that as the size of the SMAP data record increases, the accuracy of
248 the derived loss functions in these regions should increase. Also worth noting is that the
249 precipitation forecasts used herein were produced by GEOS-5, an experimental forecast system;
250 soil moisture forecasts might improve if bias-corrected precipitation forecasts from an
251 operational weather center were used instead.

252 We fully expect that many applications would benefit from more up-to-date (and forecasted) soil
253 moisture information than allowed by operational SMAP product latency. Not discussed here,
254 but also relevant, is the potential for using the approach to back-fill temporal gaps in the SMAP
255 data record – gaps caused by the unavoidable 2-3 day return time of the SMAP sensor and
256 potentially exacerbated by, for example, intermittent radio frequency interference or by active
257 rainfall during the time of overpass. Given adequate precipitation data and a suitable time period
258 over which to fit the functions, the data-driven loss function approach indeed has the potential to
259 transform the SMAP data record into a daily record of soil moisture with no missing data, all the
260 way up to real time or even a few days into the future.

261

262 *Acknowledgments.* This work was supported by NASA through its funding of the SMAP
263 Science Team (announcement NNH12ZDA001N-SMAP). We thank Qing Liu, Austin Conaty, and
264 Jana Kolassa for help with the datasets.

265

266 **References**

- 267 Brodzik, M. J., B. Billingsley, T. Haran, B. Raun, and M. H. Savoie, 2012: EASE-Grid 2.0:
268 Incremental but Significant Improvements for Earth-Gridded Data Sets. ISPRS
269 International Journal of Geo-Information, 1(1): 32-45.
- 270 Charba, J. P., and F. G. Samplatsky, 2011: High-resolution GFS-based MOS quantitative
271 precipitation forecasts on a 4-km grid. Monthly Weath. Rev., 139, 39-68.
- 272 Clark, M., S. Gangopadhyay, L. Hay, B. Rajagopalan, and R. Wilby, 2004: The Schaake Shuffle,
273 A method for reconstructing space-time variability in forecasted precipitation and
274 temperature fields. J. Hydromet., 5, 243-262.
- 275 Entekhabi, D., and Co-authors, 2010: The Soil Moisture Active Passive (SMAP) mission. *Proc.*
276 *IEEE*, 98, 704-716.
- 277 Huffman, G. J., D. T. Bolvin, D. Braithwaite, K. Hsu, R. Joyce, and P. P. Xie, 2014: NASA
278 Global Precipitation Measurement (GPM) Integrated Multi-satellitE Retrievals for GPM
279 (IMERG). Algorithm Theoretical Basis Document, Version 4.4, National Aeronautics and
280 Space Administration. Available at
281 https://pps.gsfc.nasa.gov/Documents/IMERG_ATBD_V4.pdf.
- 282 Jackson, T., and Co-authors, 2016: Soil Moisture Active Passive (SMAP) Project Calibration
283 and Validation for the L2/3_SM_P Version 3 Data Products. Jet Propulsion Laboratory,
284 California Institute of Technology, Pasadena, California. JPL Publication, JPL D-93720.

285 Koster, R. D., Z. Guo, R. Yang, P. A. Dirmeyer, K. Mitchell, and M. J. Puma, 2009: On the
286 nature of soil moisture in land surface models. *J. Climate*, 22, 4322-4335.

287 Koster, R. D., L. Brocca, W. T. Crow, M. S. Burgin, and G. J. M. De Lannoy, 2016:
288 Precipitation estimation using L-band and C-band soil moisture retrievals. *Water*
289 *Resources Research*, 52, 7213–7225, doi:10.1002/2016WR019024.

290 Manabe, S., 1969: Climate and the ocean circulation, I, The atmospheric circulation and the
291 hydrology of the Earth's surface. *Mon. Wea. Rev.*, 97, 739-774.

292 O'Neill, P. E., S. Chan, E. G. Njoku, T. Jackson, and R. Bindlish. 2016. SMAP L2 Radiometer
293 Half-Orbit 36 km EASE-Grid Soil Moisture, Version 3. Boulder, Colorado USA. NASA
294 National Snow and Ice Data Center Distributed Active Archive Center.
295 doi:10.5067/PLRS64IU03IT. Accessed June, August, and October 2016.

296 Salvucci, G. D., 2001: Estimating the moisture dependence of root zone water loss using
297 conditionally averaged precipitation. *Water Resour. Res.*, 37, 1357-1365,
298 doi:0.1029/2000WR900336.

299 Sun, J., G. D. Salvucci, D. Entekhabi, and L. Farhadi, 2011: Parameter estimation of coupled
300 water and energy balance models based on stationary constraints of surface states. *Water*
301 *Resour. Res.*, 47, W02512,doi:10.1029/2010WR009293.

302

303 **Figure Captions**

304

305 **Figure 1.** Representative results from loss function estimation. a. Left panel: derived
306 (optimized) loss function for a grid cell in southwestern New Mexico, showing, as a function of
307 volumetric soil moisture, how much of that soil moisture (shown here in $\text{m}^3 \text{m}^{-3} \text{day}^{-1}$) is
308 expected to be removed from the near surface through evaporation and drainage. Top right
309 panel: SMAP Level 2 soil moisture retrievals ($\text{m}^3 \text{m}^{-3}$) at the grid cell (red dots) and
310 corresponding simulated values obtained using the loss function in conjunction with the observed
311 CPCU precipitation data over the time period (blue dots; see text). Bottom right panel: CPCU
312 precipitation (mm day^{-1}). The x-axis on the rightmost plots begins on May 1, 2015. b. Same, but
313 for a grid cell in southwestern Kansas. c. Same, but for a grid cell in central Indiana.

314

315 **Figure 2.** Spatial distribution of the square of the correlation coefficient between the 2015
316 SMAP Level 2 soil moisture retrievals and the soil moisture estimates produced using the loss
317 functions fitted to that year's data. To generate the estimates, soil moisture at each grid cell was
318 initialized on 1 May 2015 and then updated through September using the locally optimized loss
319 function and the time series of local precipitation.

320

321 **Figure 3.** (a) Skill of 1-day lead soil moisture estimates (computed as the RMSE of estimated
322 soil moisture versus SMAP retrieval value, if it exists, one day after a given retrieval) for the loss

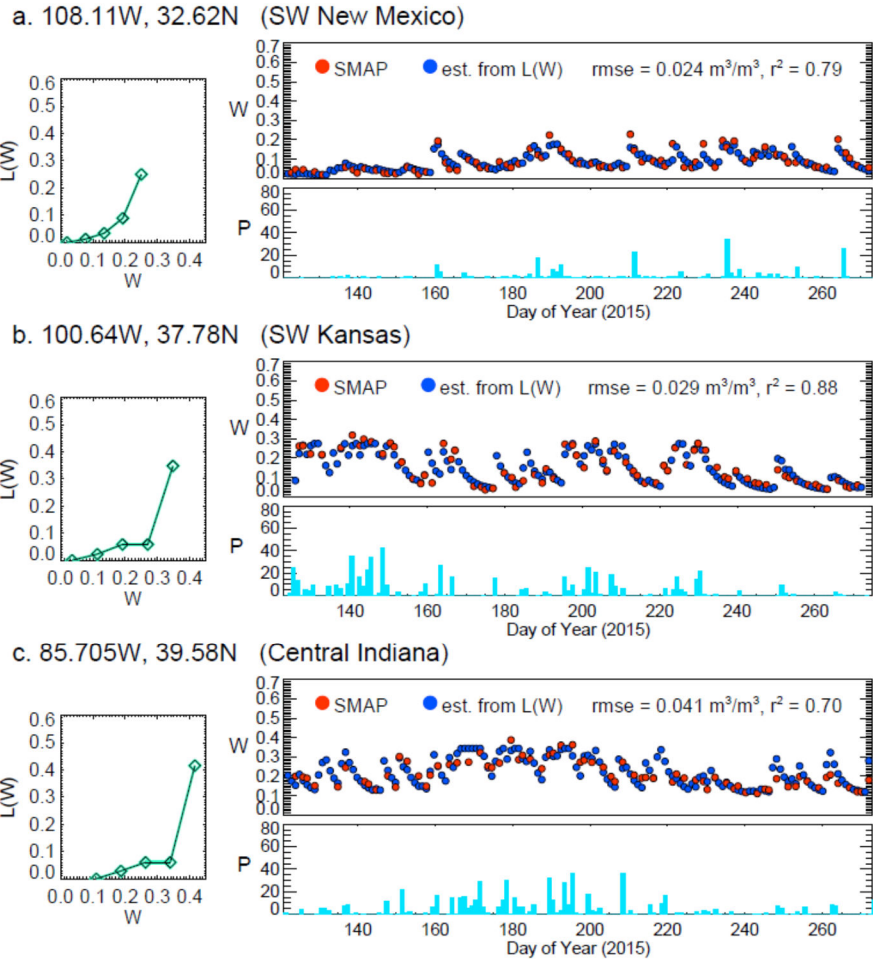
323 function approach using gauge-measured precipitation (left panel, relevant to soil moisture
324 nowcasts), the loss function approach using forecasted precipitation (middle panel, relevant to
325 soil moisture nowcasts and forecasts), and the persistence approach (right panel). Results are
326 shown for 2016, a period independent of that used to optimize the loss functions. (b) Same, but
327 for 2-day lead estimates. (c) Same, but for 3-day lead estimates. (d) Same, but for 5-day lead
328 estimates.

329

330 **Figure 4.** Areal averages of the RMSE values in Figure 3 as a function of lead for the
331 persistence approach (blue), the loss function approach using forecasted precipitation (yellow),
332 and the loss function approach using gauge-measured precipitation (red), of relevance to
333 potential nowcast calculations.

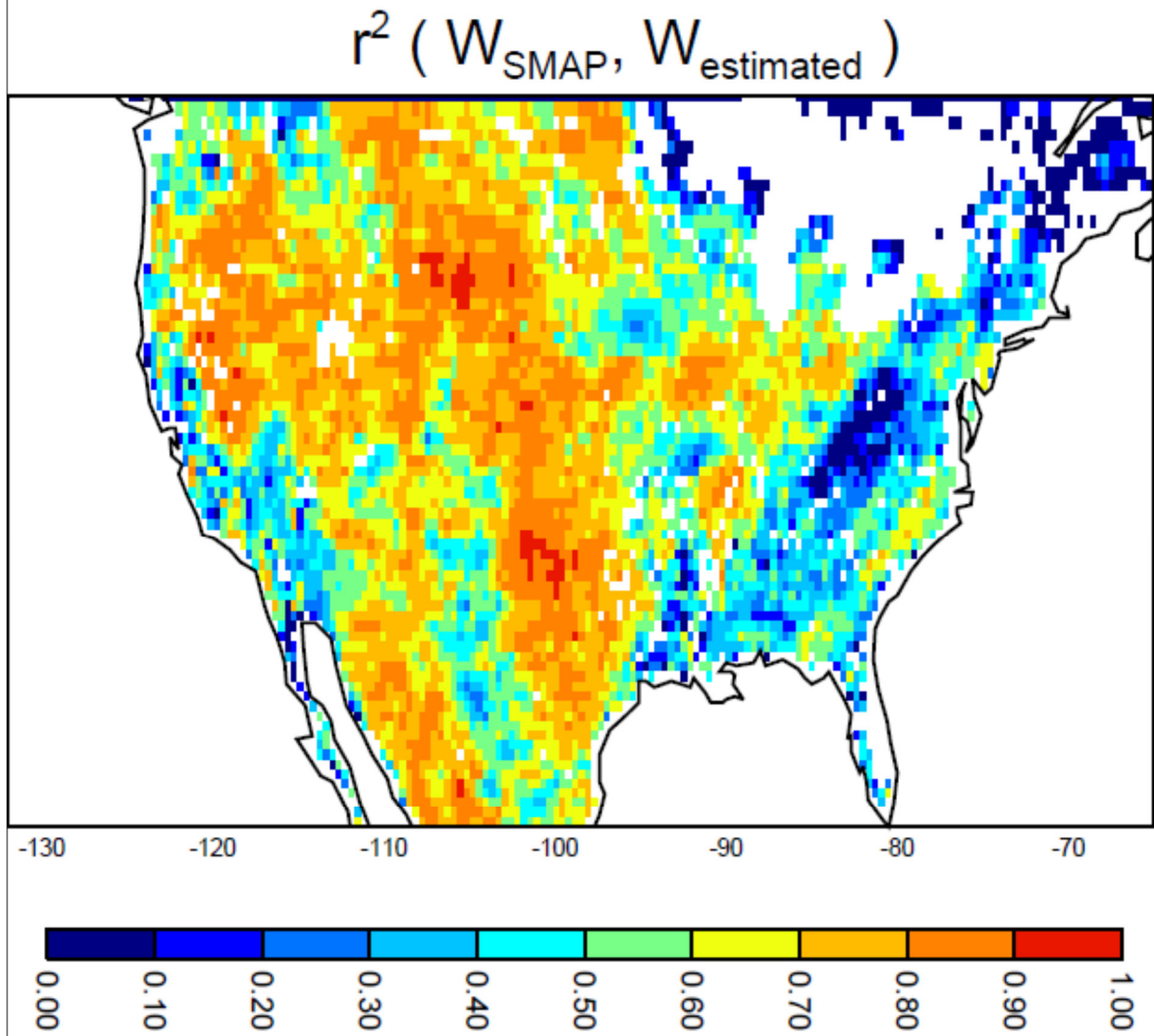
334

335



336

337 **Figure 1.** Representative results from loss function estimation. a. Left panel: derived
 338 (optimized) loss function for a grid cell in southwestern New Mexico, showing, as a function of
 339 volumetric soil moisture, how much of that soil moisture (shown here in $\text{m}^3 \text{m}^{-3} \text{day}^{-1}$) is
 340 expected to be removed from the near surface through evaporation and drainage. Top right
 341 panel: SMAP Level 2 soil moisture retrievals ($\text{m}^3 \text{m}^{-3}$) at the grid cell (red dots) and
 342 corresponding simulated values obtained using the loss function in conjunction with the observed
 343 CPCU precipitation data over the time period (blue dots; see text). Bottom right panel: CPCU
 344 precipitation (mm day^{-1}). The x-axis on the rightmost plots begins on May 1, 2015. b. Same, but
 345 for a grid cell in southwestern Kansas. c. Same, but for a grid cell in central Indiana.

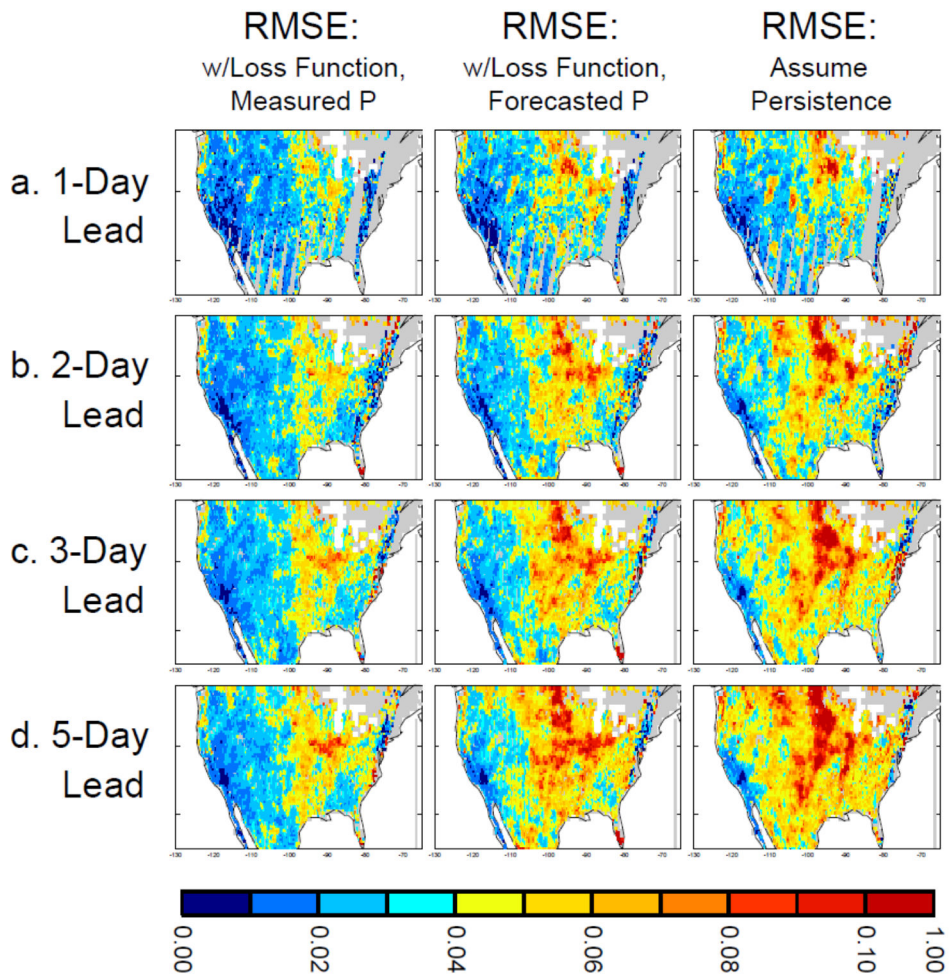


346

347

348

349 **Figure 2.** Spatial distribution of the square of the correlation coefficient between the 2015
 350 SMAP Level 2 soil moisture retrievals and the soil moisture estimates produced using the loss
 351 functions fitted to that year's data. To generate the estimates, soil moisture at each grid cell was
 352 initialized on 1 May 2015 and then updated through September using the locally optimized loss
 353 function and the time series of local precipitation.

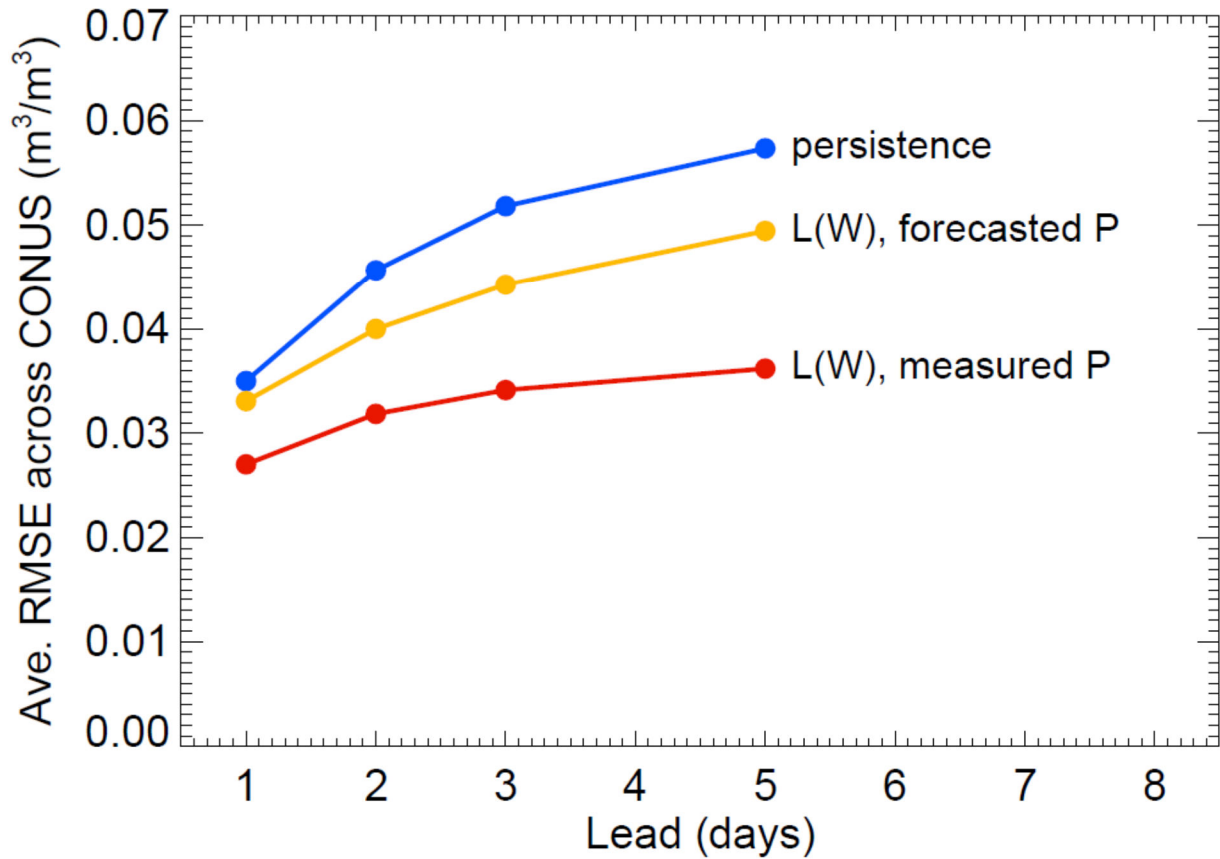


354

355 **Figure 3.** (a) Skill of 1-day lead soil moisture estimates (computed as the RMSE of estimated
 356 soil moisture versus SMAP retrieval value, if it exists, one day after a given retrieval) for the loss
 357 function approach using gauge-measured precipitation (left panel, relevant to soil moisture
 358 nowcasts), the loss function approach using forecasted precipitation (middle panel, relevant to
 359 soil moisture nowcasts and forecasts), and the persistence approach (right panel). Results are
 360 shown for 2016, a period independent of that used to optimize the loss functions. (b) Same, but
 361 for 2-day lead estimates. (c) Same, but for 3-day lead estimates. (d) Same, but for 5-day lead
 362 estimates.

363

364



365

366

367 **Figure 4.** Areal averages of the RMSE values in Figure 3 as a function of lead for the
368 persistence approach (blue), the loss function approach using forecasted precipitation (yellow),
369 and the loss function approach using gauge-measured precipitation (red), of relevance to
370 potential nowcast calculations.